

Numerical and Analytical analysis of 3D printer extruder in Fused Deposition Modelling

*Shishirkumarsingh, Prof. Rajesh K Satankar²
M.Tech scholar¹, Assistant Prof. Mechanical department²
Jabalpur Engineering College, Jabalpur*

Abstract—Fused Deposition modeling is the prime method of Additive manufacturing process used for the polymer manufacturing. As in this process the polymer filament enter in to the heat sink through feed filament feed mechanism and reaches to the heat block where it get melts and through the nozzle it get extruded and deposited layer by layer in order to build the component. In order to extrude the PLA melt, the feed polymer filament in solid form is used as a plunger. In order to use Polymer filament as a plunger, it is necessary to remain polymer filament is in solid state inside the heat sink. In order to remain feed filament in solid state it is necessary to remain the temperature of the heat sink much below the melting temperature of polymer. In order to increase the heat transfer rate from the heat sink it is necessary to increase the surface area of heat sink. Therefore in order to increase the surface area of heat sink, fins are provided on the heat sink. Here in this work thermal behavior of heat sink is analyzed. Here it also contains the optimization of heat sink fins profile, in this analysis heat sink having circular, triangular, elliptical and rectangular having elliptical perforation fin are analyzed for working material that is poly-lactic-acid (PLA). It also finds out the effect of pressure drop inside the liquefier and calculates the optimum pressure drop inside the liquefier through analyzing the 27 combinations of nozzle angle and nozzle diameter.

1. Introduction

The term 3D printing covers a host of processes and technologies that offer a full spectrum of capabilities for the production of parts and products in different materials. Essentially, what all of the processes and technologies have in common is the manner in which production is carried out layer by layer in an additive process which is in contrast to traditional methods of production involving subtractive methods or moulding/casting processes. Applications of 3D printing are emerging almost by the day, and, as this technology continues to penetrate more widely and deeply across industrial, maker and consumer sectors, this is only set to increase. Most reputable commentators on this technology sector agree that, as of today, we are only just beginning to see

the true potential of 3D printing. 3DPI, a reliable media source for 3D printing, brings you all of the latest news, views, process developments and applications as they emerge in this exciting field. This overview article aims to provide the 3DPI audience with a reliable backgrounder on 3D printing in terms of what it is technologies, processes and materials, its history, application areas and benefits.

Kousiatza et.al The present work investigates the integration of fibre Bragg grating (FBG) sensors for continuous in-situ and in real-time monitoring of strain fields. Szykiedans et.al a new development of the 3-D printers, which has made them freely existing to the public at low costs. In order to make 3-D printed parts to be more useful for engineering applications the mechanical properties of the printed parts to be known must. Casavola et.al The Fused Deposition Modeling (FDM) has become one of the most used techniques to 3D object rapid prototyping. In this process, the model is built as a layer-by-layer deposition of a feedstock wire. Jerez-Mesa et.al the aim of this paper is to analyses the performance of a RepRap 3D printer liquefier by studying its thermal behavior, concentrating on the convective heat dissipation developed beside the liquefier body all through the 3D printing process of a workpiece. Yifan Jin et.al Fused deposition modeling has become one of the most diffused rapid prototyping techniques, which is widely used to fabricate prototypes. On the other hand, further application of this technology is rigorously affected by poor surface roughness mainly due to staircase effect.

2. Material Used

Thermal properties of the materials (PLA, aluminum and brass) are taken from literature survey and used in this analysis. The thermal conductivity of PLA is assumed to be constant as 0.195 W/m-K [25]. Specific heat capacity for PLA as a function of temperature is determined by Pyda et al. [21] based on differential scanning calorimetric and adiabatic calorimetric. The temperature and specific heat capacity relationship of PLA are based on the work of Pyda et al. [21] (for a molar mass of 72.06 g/mol) and are provided in table 1. It is shown that the specific heat capacity of PLA in FDM follows two different approximately linear portions for temperatures above and below 332.5 K, which is stated to be the glass transition temperature. Within the model the temperature dependent values based on Fig. are used. For temperature below than 332.5 K, the specific heat capacity is assumed to be $(4.4T + 58)$ J/Kg-K and for 332.5 K and above, the specific heat capacity value is assumed to be $(1.05 T + 1668)$ J/Kg-K

Table.1 Showing the value of material properties of PLA

Thermal Property of PLA	Value
Specific Heat	(1.05 T + 1668)
Thermal conductivity k	0.19 W/m K
Solidification Temperature	448 K
Melting temperature	448 K
Viscosity	Follow Power law
Density	1250 m^3 / Kg
Enthalpy of melting	45000 J/Kg

- Properties for Brass material

Table 1 showing the material properties of Brass

Thermal property	Value
Thermal conductivity (K)	109 W/m-k
Specific heat (C_p)	380 J/kg-k
Density (ρ)	9490 kg/m^3

- Properties for Aluminum material

Table 3. Showing the material property of aluminium

Thermal property	Value
Thermal conductivity (K)	237 W/m-k
Specific heat (C_p)	903 J/kg-k
Density (ρ)	2702 kg/m^3

3. Development of CFD model

In order to find out the temperature distribution throughout the extruder, it is necessary to develop the CFD model of extruder and apply different boundaries measured during the experimental analysis perform by different researcher. Here in this analysis first it develops the CFD model of extruder and then it optimizes the geometry of heat sink, because the design of

heat sink is completely based on the temperature distribution. The temperature at the heat sink must remain low as much as possible.

3.1 Solid model of 3D printer extruder

The CFD model used can be solved numerically solution using input conditions and applying governing conservation of mass, momentum and energy to each specific part of the body. For this model, the primary steady-state boundary conditions include a constant inlet velocity applied where the ridge PLA filament is fed into the heater barrel assembly, an outlet pressure applied at the dispensing orifice of the nozzle, a heat generation body where the heater cartridge is present within the heater block and the heat transfer coefficient applied on the external surfaces of the component. Since the initial inner diameter of the groove mount and heat barrel are slightly larger than the PLA filament diameter, mass flow rate equation is used to adjust the inlet velocity of the model to match the filament speed as it enters the system.

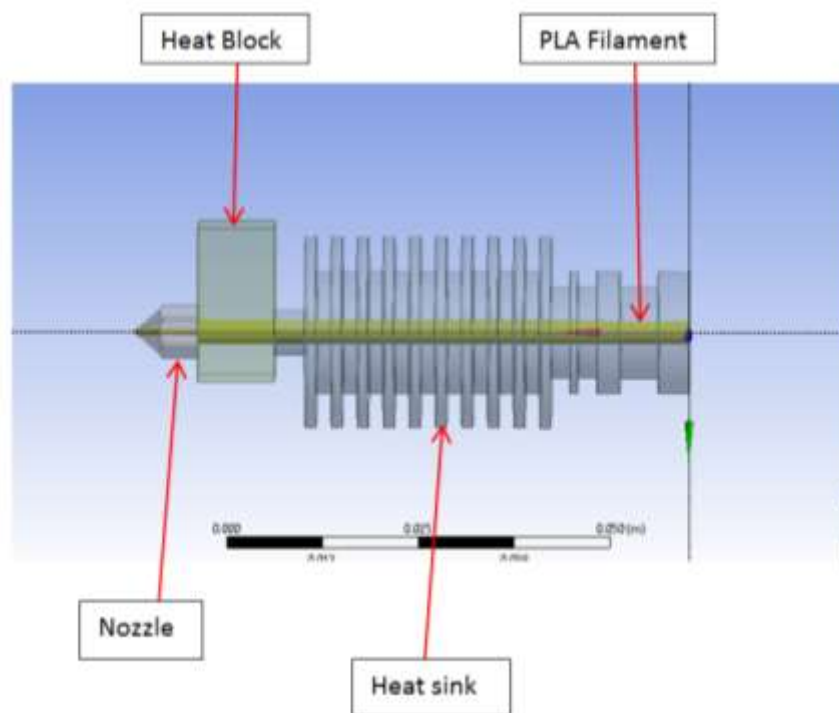


Fig.1 Complete solid model of liquefier with PLA space filled

3.2 Calculating analytically Heat transfer coefficient

Convection and radiation within the heat sink, heat block and nozzle is accounted for calculating the effective heat transfer coefficient on the exterior surfaces of the components. By using the equation for effective heat transfer equation as we mention (i.e $h_{effective}$).

$$h_{effective} = h_{convection} + h_{radiation}$$

The effective heat transfer coefficient is calculated by adding the convective heat transfer coefficient and radiation heat transfer. Following values (Table 4.4) at different sections of component are applied at the exterior surface of component as a boundary condition within the fluid dynamic solver.

Table 4. Effective Heat Transfer coefficient values at different surfaces of components

Face location	$h_{convection}$ (W/m ² K)	$h_{radiation}$ (W/m ² K)	$h_{effective}$ (W/m ² K)
Heat sink	10.3	3.2	13.5
Heat block top	20.1	3.3	23.4
Heat block sides	11.9	3.3	15.2
Heat block bottom	13.8	3.3	17.1
Nozzle	19.6	3.2	22.8

3.3 Meshing

Different meshing approaches used for this model are the insertion of a relevant center, inflation, body sizing, and assembly mesh. The simulation is run using three separate mesh to guarantee mesh independence. The mesh independence is based on the outlet mass flow average temperature and the meshed model is depicted through figure

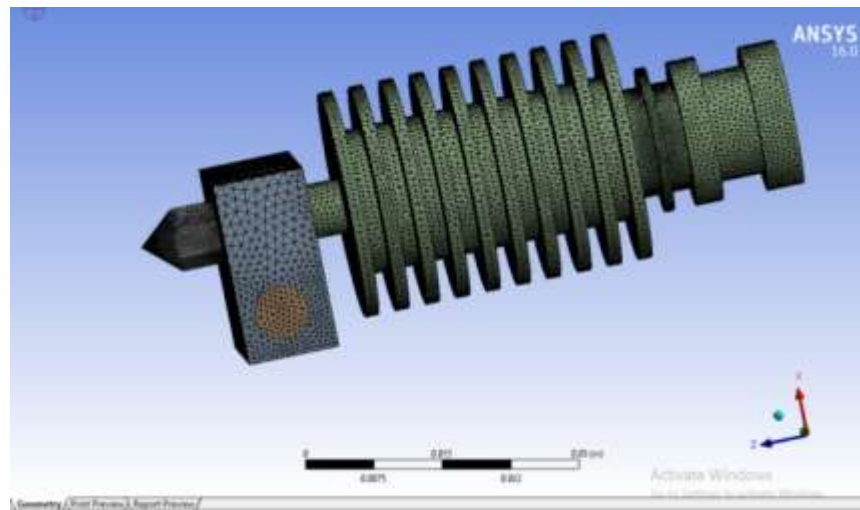


Fig.2 Meshing of FDM Liquefier

3.4 Boundary conditions

The procedure that is followed during the solution method are shown in fig.4.20 Here pressure based solver is used. The pressure-based solvers take momentum and pressure (or pressure correction) as the primary variables. Pressure-velocity coupling algorithms are derived by reformatting the continuity equation. The pressure-based solver is applicable for a wide range of flow regimes from low speed incompressible flow to high-speed compressible flow. The pressure-based coupled solver (PBCS) is applicable for most single phase flows, and yields superior performance as compared to the pressure-based (segregated) solver

4. Result

As the aim of presented simulation is to successfully model all the heat transfer mechanism and their effect on the component of the system, the steps are primarily focused on the temperature profile of the melt PLA that includes flow inside the liquefier as well as external temperature of the heat block, heat sink and nozzle. Figure 4.28 shows an image of the overall temperature profile of the entire system.

4.1 For extruder having the circular fins

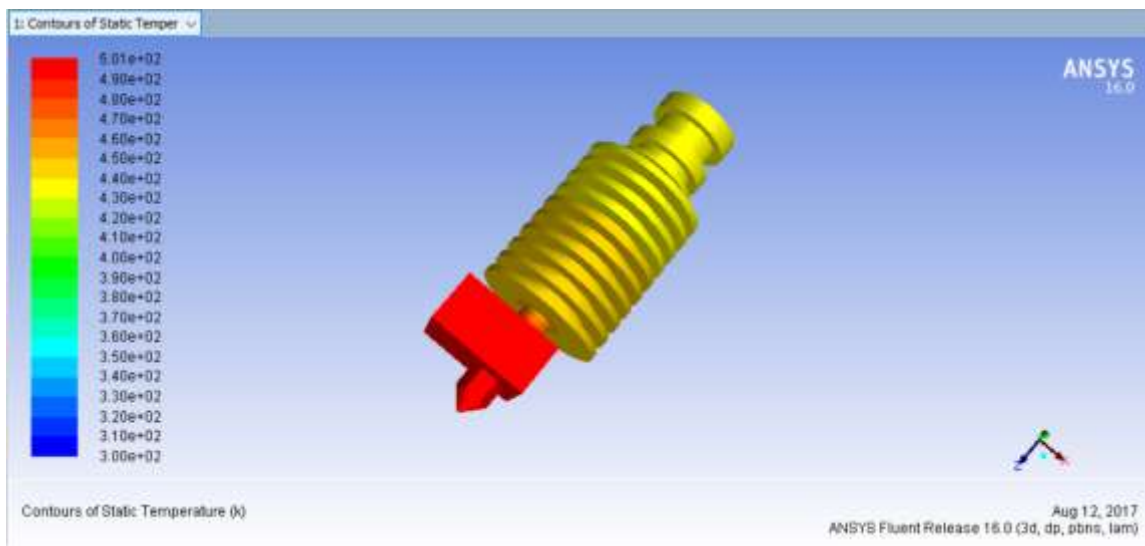


Fig. 3 liquefier temperature gradient

The variation of temperature throughout the PLA polymer from inlet of PLA filament at liquefier entrance to the extruded melt at the nozzle exit is shown in figure 4.29.

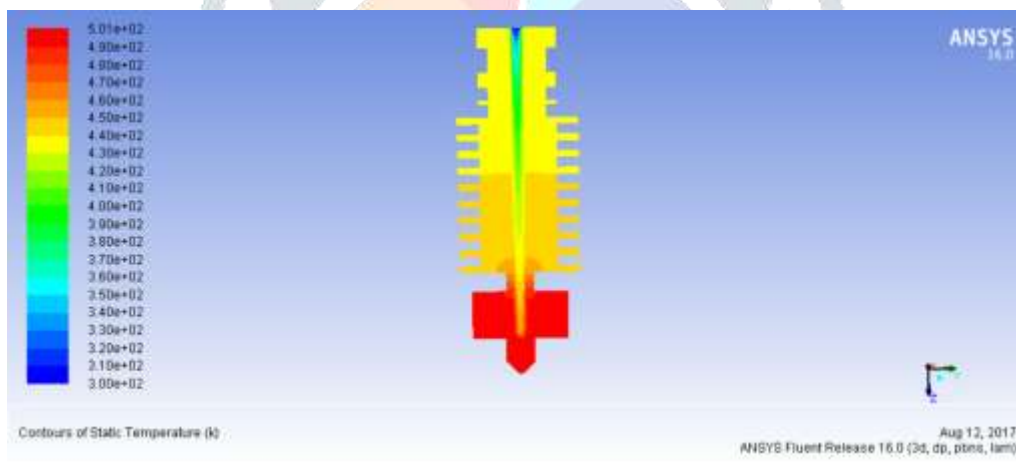


Fig.4 showing the temperature distribution throughout the extruder of heat sink

Figure 4.29 shows that the temperature along the outside of the polymer melt also goes on changing. The top portion of heat sink has temperature of about 440 K whereas the middle section reaches up to more than 445 K. At the end of the nozzle where material is deposited the temperature is about 490 K. This variation can serve as an important consideration for modeling and simulating the behavior of melting.

4.2 For Extruder having triangular fins

As it has calculated the temperature distribution in the circular heat sink applying the different boundary conditions, by applying the same boundary condition it can also find out the temperature distribution inside the heat sink having triangular fins at same velocity of air. The temperature contour for triangular heat sink is shown in the fig.4.31.

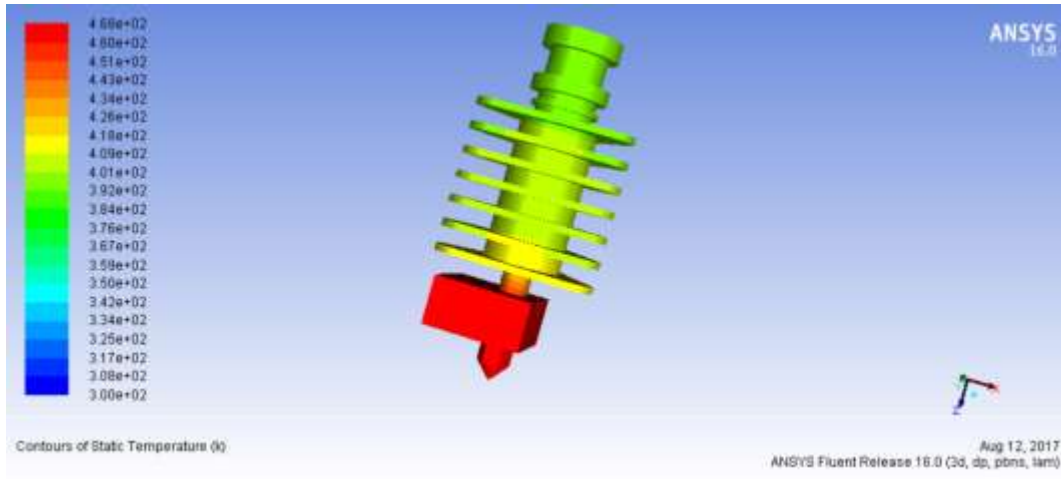


Fig.5 showing the temperature distribution for triangular fins heat sink

With the help of above analysis it is observed that the temperature of heat sink at the top most position is near about 405 K.

4.3 For extruder having Elliptical fins

Temperature distribution inside the extruder having elliptical fins is calculated based on the boundary condition used during the analysis of extruder having the circular fins.

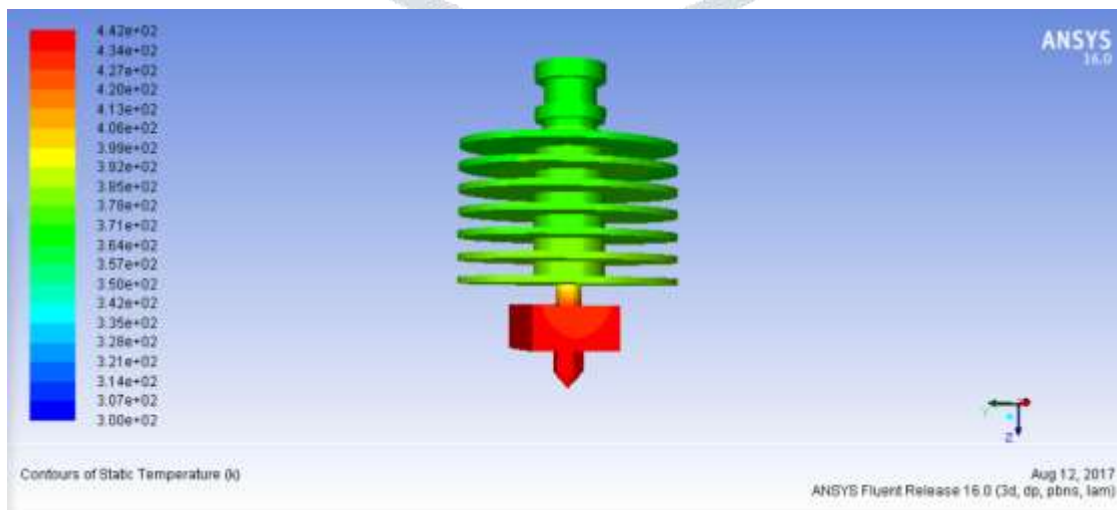


Fig. 6 showing the temperature distribution throughout the heat sink having the elliptical fin

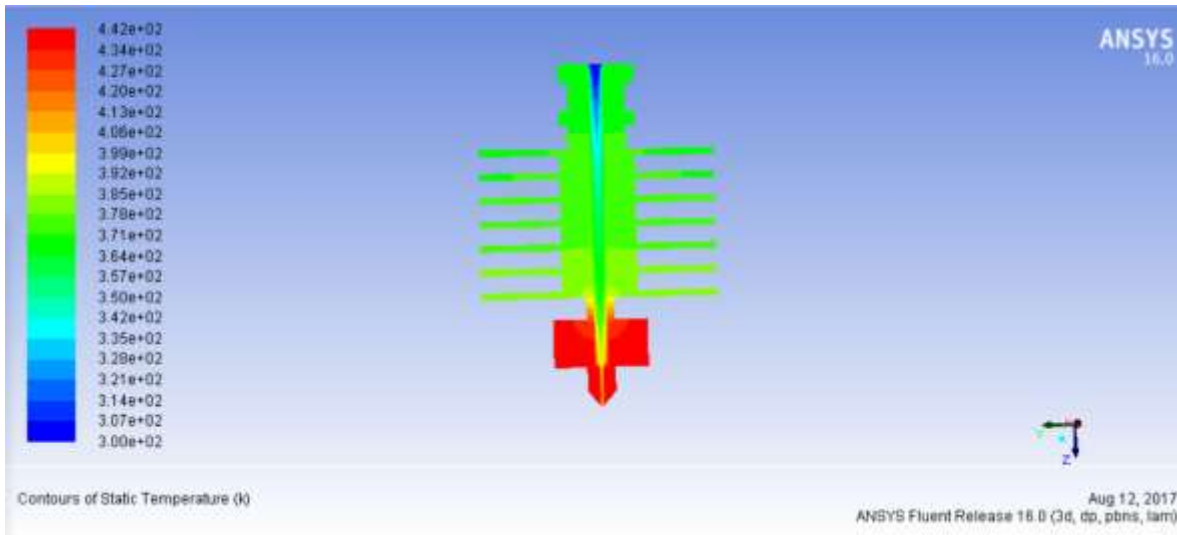


Fig. 7 showing the section view of extruder having the elliptical fins

From the above analysis it is observed that the temperature at top of the elliptical fins is near about 380 K.

4.4 Rectangular with elliptical perforation fins.

Temperature distribution inside the extruder having rectangular with elliptical perforation fins is calculated based on the boundary condition measured during experimental analysis is shown in the fig.

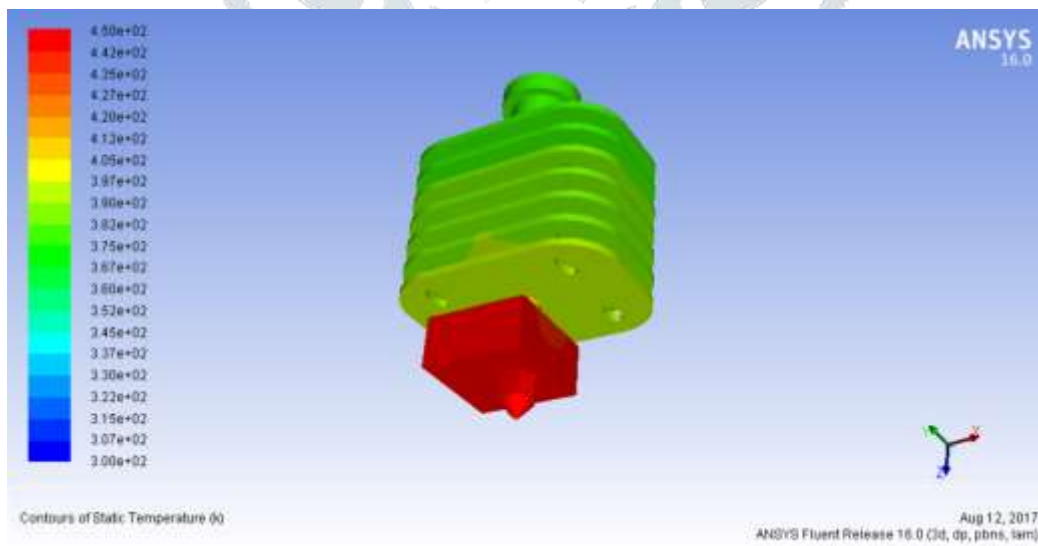


Fig.8 showing the temperature distribution of extruder having the rectangular with elliptical perforation fins

From the above analysis it is observed that temperature at the top of the heat sink is near about 370 K which is quite under the desirable conditions and it is also less as compared to the other design of heat sink. Therefore heat sink having the rectangular with elliptical fins is showing the optimum temperature required at the top of the heat sink. It also shows the desirable temperature variation throughout the liquefier. To melt the PLA filament temperature required at the heat block can be increased by increasing the supply to the heat cartridge, through this cartridge it can achieve the desire temperature at the heat block and nozzle. Due to the increased of surface area in the rectangular having elliptical perforation rate of heat transfer get increased, due to this low temperature raise in heat sink and PLA filament maintained in the solid form.

5. CONCLUSION

Through CFD analysis it can find the temperature distribution through the extruder which helps in design of extruder geometry. Simulating the 3D printer liquefier heat sink having different shaped fins that is circular, triangular, elliptical and rectangular having elliptical perforation. From the above result it is found that the rectangular fins having elliptical perforation has least temperature distribution. Through different extruder analysis it is finding that the temperature distribution inside the extruder is a critical parameter for doing the 3D printing. Surface finishing of the 3D printed component depends on the consistency of the extruded material whereas the consistency of the extruded material depends on the temperature and pressure drop inside the extruder.

REFERENCE

- 1) Yifan Jin, Yi Wan, Bing Zhang, Zhanqiang Liu, Modeling of the chemical finishing process for polylactic acid parts infused deposition modeling and investigation of its tensile properties, *Journal of Materials Processing Technology* 240 (2017) 233–239.
- 2) Ksawery Szykiedans, Wojciech Credo, Mechanical properties of FDM and SLA low-cost 3-D prints, *Procedia Engineering* 136 (2016) 257 – 262.

- 3) CaterinaCasavola, Alberto Cazzato, Vincenzo Moramarco, Carmine Pappalettere, Orthotropic mechanical properties of fused deposition modelling parts described by classical laminate theory, *Materials and Design* 90 (2016) 453–458.
- 4) R. Jerez-Mesa , J.A. Travieso-Rodriguez , X. Corbella , R. Busque, G. Gomez-Gras, Finite element analysis of the thermal behavior of a RepRap 3D printer liquefier, *Mechatronics* 0 0 0 (2016) 1–8.
- 5) CharoulaKousiatza, DimitrisKaralekas, In-situ monitoring of strain and temperature distributions during fused deposition modeling process, *Materials and Design* 97 (2016) 400–406.
- 6) ZixiangWeng, Yu Zhou, Wenxiong Lin, T. Senthil, Lixin Wu, Structure-Property Relationship of Nano Enhanced Stereolithography Resin for Desktop SLA 3D Printer, *S1359-835X(2016)30172-5*.
- 7) M. N. Islam & Samuel Sacks, An experimental investigation into the dimensional error of powder-binder three-dimensional printing, *Int J AdvManufTechnol* (2016) 82:1371–1380.
- 8) L. M. Galantucci, I. Bodi, J. Kacani, F. Lavecchia, Analysis of dimensional performance for a 3D open-source printer based on fused deposition modeling technique, *Procedia CIRP* 28 (2015) 82 – 87.
- 9) Andreas Eitzlmayr, Johannes Khinast, Co-rotating twin-screw extruders: Detailed analysis of conveying elements based on smoothed particle hydrodynamics. Part 1: Hydrodynamics, 0009-2509/& 2015 Elsevier Ltd.
- 10) Dawei Li & Ning Dai & Xiaotong Jiang & Xiaosheng Chen, Interior structural optimization based on the density-variable shape modeling of 3D printed objects, *Int J AdvManufTechnol* 20 March 2015
- 11) Kyung Tae Lee, Eun-Seob Kim, Won-Shik Chu and Sung-HoonAhn, Design and 3D printing of controllable-pitch archimedean screw for pico-hydropower generation, *Journal of Mechanical Science and Technology* 29 (11) (2015) 4851~4857.
- 12) Garrett W. Melenka and Jonathon S. Schofield, Evaluation of dimensional accuracy and material properties of the MakerBot 3D desktop printer, *Rapid Prototyping Journal* 21/5 (2015) 618–627.
- 13) O.S. Carneiro, A.F. Silva , R. Gomes, Fused deposition modeling with polypropylene, *Materials & Design* 83 (2015) 768–776.

- 14) Yang Yang & Yonghua Chen & Ying Wei & Yingtian Li, 3D printing of shape memory polymer for functional part fabrication, Int J AdvManufTechnol 10 March 2015.
- 15) Mohammad Taufik, Prashant K. Jain, A Study of Build Edge Profile for Prediction of Surface Roughness in Fused Deposition Modeling, JUNE 2016, Vol. 138 / 061002-1.
- 16) N. Volpato & D. Kretschek & J. A. Foggia & C. M. Gomez da Silva Cruz, Experimental analysis of an extrusion system for additive manufacturing based on polymer pellets, 4 February 2015.
- 17) Samuel R. Stewart, John E. Wentz, Joseph T. Allison, EXPERIMENTAL AND COMPUTATIONAL FLUID DYNAMIC ANALYSIS OF MELT FLOW BEHAVIOR IN FUSED DEPOSITION MODELLING OF POLY(LACTIC) ACID, November 13-19, 2015, Houston, Texas.
- 18) Huhn Kim and Seongwon Jeong, Case study: Hybrid model for the customized wrist orthosis using 3D printing, Journal of Mechanical Science and Technology 29 (12) (2015) 5151~5156.
- 19) A. Boschetto & L. Bottini, Accuracy prediction in fused deposition modelling, 11 December 2013, 9 May 2014.
- 20) Xuan Li, ChaoGuo, XiaokaiLiu, LeiLiu, JingBai, FengXue, PinghuaLin, ChenglinChu, Impact behaviors of poly-lactic acid based biocomposite reinforced with unidirectional high-strength magnesium alloy wires Progress in Natural Science: Materials International 24(2014)472-478.
- 21) B. Pyda, M., Bopp, R. C., & Wunderlich, B. (2004). Heat capacity of poly (lactic acid). The Journal of Chemical Thermodynamics, 36(9), 731-742.
- 22) C. Djellali, S., Sadoun, T., Haddaoui, N., and Bergeret, A. Viscosity and viscoelasticity measurements of low density polyethylene/poly (lactic acid) blends. Polymer Bulletin, 72(5), 1177-1195.
- 23) Incropera, F. P. (1996). Introduction to heat transfer. John Wiley & Sons.
- 24) Bellini, A. (2002). Fused deposition of ceramics: a comprehensive experimental, analytical and computational study of material behavior, fabrication process and equipment design. (Doctoral dissertation, Drexel University)
- 25) Zehevtadmor, Costas G. gogos, principles of polymer processing, A John Wiley & Sons, Inc., Publication.

- 26) Jamshidian, M., Tehrany, E. A., Imran, M., Jacquot, M., and Desobry, S. (2010). Poly- lactic acid: production, applications, nanocomposites, and release studies. *Comprehensive Reviews in Food Science and Food Safety*, 9(5), 552-571.
- 27) McKelvey, J.M., *Polymer Processing*, Wiley, New York, 1962.
- 28) Norton, R. L. *Machine Design: An Integrated Approach*. Prentice Hall, 2000.

